Base Station Deployment Optimization in Integrated Access and Backhaul Networks Using Evolutionary Algorithms

Fco. Italo G. Carvalho, Igor B. Palhano, Tarcisio F. Maciel, Raul V. de O. Paiva

***Abstract*— Integrated access and backhaul networks are a good solution for fifth gerantion networks, due to its potential to increase the bandwidth used for wireless connections and a low implementation cost compared to other solutions. In order to solve the problem of positioning bases, in the proposed work we optimized an Integrated access and backhaul network to increase the spectral efficiency for different proportions of macros and small base stations and, for this, we used genetic algorithm and particle swarm optimization. The results obtained show that for all scenarios it is possible to obtain a high spectral efficiency, however, for scenarios with low proportions of small base stations, genetic algorithm shows high performance, while in the scenario of high proportions particle swarm optimization converges to values close to those of genetic algorithm. Thus, we conclude that the algorithms used solve the proposed problem and that for a high proportion of small base station, particle swarm optimization becomes an attractive solution due to its high proximity to the results obtained via genetic algorithm and its lower computational complexity.**

***Keywords*— Integrated access and backhaul, 5G-NR, base station deployment, evolutionary algorithms, spectral efficiency**

I. Introduction

The sustained expansion of data traffic over time, primarily propelled by the ongoing widespread adoption of smartphones and a rising average data volume per subscription has been fueling fifth gerantion (5G) network growth. Between the fourth quarter of 2022 and the fourth quarter of 2023, mobile data traffic grew 28%, reaching almost 1.6 billion subscriptions worldwide [1].

To aid 5G deployment in meeting the increasing demand for high-speed data transmission, Integrated access and backhaul (IAB) networks are particularly relevant, providing more flexible and scalable solutions due to their cost-effectiveness and fast deployment [2]: This is achieved due to their wireless communication infrastructure, designed to efficiently support access and backhaul functionalities, which traditionally have been deployed separately, within a single network architecture, reducing costly and some times unfeasible wired network infrastructures.

For instance, the wireless backhaul capability of long term evolution (LTE) networks has been deemed not flexible enough, as it only allows for a rigid allocation of the resources, with the relay [3] associated with a fixed parent base station (BS) [4]. However, this separation can lead to infrastructure deployment, management, and utilization inefficiencies.

IAB, in the context of 5G networks, empowers the usage of radio resources for backhaul by making use of the wider bandwidths of millimeter wave (mmWave) paired with the directivity of massive multiple-input multiple-output (MIMO), providing higher transmit rates, and also enabling multihop, flexible topology and dynamic resource sharing [2].

Still, employing a wireless backhaul brings many challenges, such as making the network potentially more vulnerable to propagation phenomena. These losses however can be mitigated by proper network planning in order to achieve suitable cost-benefit trade-offs [5].

More commonly, in IAB networks the macro base stations (MBSs) are referred to as IAB donors, representing not only their higher transmission power but also their connection to the core network (CN) by a wired backhaul and their backhaul providing capabilities to the small base stations (SBSs), therefore called IAB nodes due to their lower transmission power and wireless backhaul, as in [2], [5], [6]. For a more detailed discussion about IAB networks see [2].

To analyze the cost-benefit balance between IAB donors and IAB nodes, we evaluate different deployment scenarios with varying positioning and IAB nodes to IAB donors ratios, since they play a crucial role in ensuring quality of service [5]. Optimization techniques such as evolutionary algorithms (EAs) have then been used to optimize network planning, offering efficient solutions based on network metrics.

The work presented in [7] shows a single objective optimization problem (SOOP) for network power allocation in IAB networks, obtaining good results in a two-hop scenario with 28 GHz center frequency. In [6], the authors show that it is also possible to use genetic algorithm (GA) to optimize an IAB network in a propagation scenario similar to the one presented in [7]. Here the authors show the vital importance of base station deployment (BSD) for IAB networks, as well as demonstrate that it is possible to use EA techniques to solve the BSD problem.

In [8], the authors' main objective was to demonstrate that particle swarm optimization (PSO) has reasonable performance for positioning several BSs in a real urban scenario, considering the combination of capacity and network balance as maximization criteria.

In [5], a GA was used to optimize BSD and compare the cost-benefit of IAB in four different scenarios with varying percentages of IAB donors and IAB nodes, as well as varying the total amount of BSs.

The present work is meant as a continuation study to [5].

F. I. G. Carvalho, I. B. Palhano, and T. F. Maciel, Raul V. de O. Paiva, Teleinformatics Engineering Department, UFC, Fortaleza, Brazil, email: italoguedes@alu.ufc.br,igor.palhano@alu.ufc.br,maciel@ufc.br, raul.paiva@alu.ufc.br. This work was financed in part by the Coordenação de Aperfeiçoamento de Pessoal de Nível Superior – Brasil (CAPES) – Finance Code 001. The authors acknowledge the partial support of FUNCAP/Universal under grant no. UNI-0210-00043.01.00/23 and INCT-Signals/CNPq under grant no. 406517/2022-3. T. F. Maciel was partially supported by CNPq under grant 312471/2021-1.

Here we also analyze the planning of IAB networks using EAs, but primarily focusing on the suitability of different optimization algorithms as BSD planning tools and under new conditions, namely user equipment (UE) hotspots instead of uniform random positioning, and a more rigorous channel model. In [6], [7] IAB networks are studied more thoroughly but only using GA, in [9] the authors evaluate PSO for BSD optimization in a metropolitan area, while in this work we focus mainly on the BSD of IAB networks using both GA and PSO as well as comparing their performances.

The remainder of this article is organized as follows. Section II describes our adopted system model, including the scenario in Subsection II-A, the channel model in Subsection II-B and the optimization algorithms used in Subsection II-C. Section III presents our simulation assumptions and the analyses of the obtained results. Finally, in Section IV, we draw some conclusions about the results and discuss future perspectives.

II. System Model

A. Scenario

In this work, a 5G network is deployed to provide communication service in a region R of area $L \times L$ square meters, to a number K of UEs, a fraction of which will form N circular hotspots with radius r and UE density λ in the region R, while the remaining UEs will be distributed uniformly according to Algorithm 1. The hotspot positioning Algorithm 1 works by sorting the hotspot UEs positions around N randomly select non-hotspot UEs. Fig. 1 shows a network deployment generated after the optimization process where there are 3 UE hotspots showed as a Voronoi diagram [10].

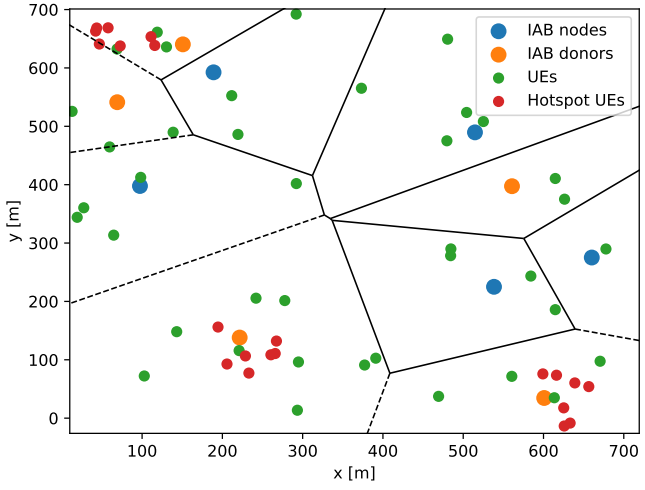

Fig. 1. An IAB network deployment is shown as a Voronoi diagram of the IAB donors and nodes with the inside and outside hotspot UEs.

We consider that the network has several cells $C = B + I$, where B are the cells served by IAB donors, connected directly to the CN through a wired backhaul and I are the cells served by IAB nodes, which deploy wireless backhaul therefore connecting to an IAB donor itself to provide communication service to its UEs. In this work, only single-hop and two-hop connections are considered, meaning a UE either connects directly to an IAB donor or connects to a single IAB node that, in turn, connects to an IAB donor.

Algorithm 1 Hotspot generation.

procedure HOSTSPOT POSITIONING(K, N, λ, r)
  n_UEs $\leftarrow \lambda \cdot r/N$; ▷ number of UEs per hotspot.
  UEs = K − *n_UEs positions;* ▷ Non-hotspot UEs
  $i \leftarrow 0$;
  while $i < N$ **do** ▷ iterate through hotspots
    pos ← *random position of UEs;*
    while j < n_UEs **do**
      rp ← *random position;*
      UEs ← *append pos+rp with |pos-rp| < r;*
      $j \leftarrow j + 1$;
    end while
    $i \leftarrow i + 1$;
  end while
end procedure

B. Channel Model

Let $h_{k,m}$ be the channel coefficient for every link between k-th UE and m-th BS. We assume that the UE will be connected to the closest BS, and it is completely transparent to the UE whether it is an IAB donor or an IAB node and every BS and UE has one antenna. The interaction between UEs and BSs in the first and second hop ares as in [5]. Let d be the distance between the k-th UE and the m-th BSand d_1 and d_2 be two threshold distances, the average path loss on logarithmic scale $L_{k,m}(d)$ is generated as

$$\begin{aligned} L_{k,m}(d) &= -140.7 - 15\log_{10}(d_2) - 20\log_{10}(d_1), \text{if } d \leq d_1, \\ L_{k,m}(d) &= -140.7 - 15\log_{10}(d_2) - 20\log_{10}(d), \text{ if } d_1 \leq d_{k,m} \leq d_2, \\ L_{k,m}(d) &= -140.7 - 35\log_{10}(d), \text{ if } d \geq d_2. \end{aligned} \quad (1)$$

In this work, we utilized correlation shadowing on a logarithmic scale $G_{\chi_{k,m}}$ for each k UE and m BS, similar to the model used in [11, Section 4], with shadowing standard deviation σ_s. Let $\zeta_{k,m}$ be the large-scale fading variable in logaritimic scale for the k-th UE and m-th BS constructed as

$$\zeta_{k,m} = L_{k,m}(d) + G_{\chi_{k,m}}. \quad (2)$$

Let $\psi_{k,m}$ be the large scale fading $\zeta_{k,m}$ in linear scale (i.e, $\psi_{k,m} = 10^{\frac{\zeta_{k,m}}{10}}$). The correlation matrix $\mathbf{R}$ will be constructed as presented in [12, eq. 2.18]

$$R_{k,m} = \psi_{k,m} \int_{-\pi}^{\pi} e^{j2\pi d_{k,m}\cos(\theta)} d\theta, \quad (3)$$

where θ is the azimuth angle and $R_{k,m}$ is the correlation element between the k-th UE and the m-th BS. Finnaly, in this work we consider only the Rayleigh fading $h_{k,m}$, therefore obtained by the product of $R_{k,m}$ and a Rayleigh-distributed variable with standard deviation σ_f

$$h_{k,m} = R_{k,m}\mathcal{R}(\sigma_f). \quad (4)$$

Following [5], the proposed signal to interference-plus-noise ratio (SINR) is modeled as

$$\gamma_{t,r} = \frac{p_{t,r} g_{t,r}}{\sum_{t' \neq t} p_{t',r} g_{t',r} + \sigma_n^2}, \tag{5}$$

where σ_n is the noise standard deviation, $g_{t,r}$ and $p_{t,r}$ represent the link gain and transmission power between the t-th BS and r-th UE.

As in [5], in order to make comparisons fair, the link capacities are considered per hop. Let $\kappa = \{1, 2, \ldots, K\}$ be the set of UEs, $\beta = \{1, 2, \ldots, B\}$ and $\Upsilon = \{1, 2, \ldots, I\}$ be the sets of IAB donors and nodes respectively, therefore $\zeta = \beta \cup \Upsilon = \{1, 2, \ldots, C\}$ is the set of BSs. In the first hop t, $t' \in \beta$ and $r \in \Upsilon \cup \kappa$, the IAB donors transmit while their UEs and the closest IAB nodes receive, and for the second hop t, $t' \in \zeta$ and $r \in \kappa$, meaning IAB donors and nodes transmit to their UEs.

To calculate the capacity $C_{t,r}$ of each link, Shannon's formula is used [13]. Let $C_{t,r}^{(1)}$ and $C_{t,r}^{(2)}$ be the channel capacities of the first and second hops, respectively, for UEs connected to IAB donors, $t \in \beta$ and $r \in \kappa$, the channel capacity is defined as

$$C_{t,r} = \frac{C_{t,r}^{(1)} + C_{t,r}^{(2)}}{2}. \tag{6}$$

For UEs connected to IAB nodes, $t \in \Upsilon$ and $r \in \kappa$, the bottleneck between the two links, either IAB donor to IAB node or IAB node to UE, is considered as shown in (7).

$$C_{t,r} = \min\{C_{t,r}^{(1)}, C_{t,r}^{(2)}\}. \tag{7}$$

C. Optimization Algorithms

Network planning is vital to guarantee good quality of service (QoS) for IAB networks. Therefore, investigating different planning tools' suitability not only in terms of high-quality solutions and effectiveness but also complexity and efficiency is imperative. Two EAs are then used to optimize BSD and give the highest spectral efficiency (SE), namely GA, and PSO, considering their intuitivety and ease of use [14], [15].

An EA, is a computational model of a natural evolution process designed to solve problems [14]. It works by having a population P of structures, possible solutions to a problem, which changes mimicking a natural process as to find even better solutions. For that purpose, each individual, one of such structures, is measured in terms of how well it solves the considered problem by means of its fitness $f_{fit}(\cdot)$.

GAs is a branch of EAs that can be defined as a global optimization technique based on the biological process of evolution [14]. Based on the fitness metric, the natural selection process includes the population in order to simulate the survival of the fittest through the genetic operators, namely reproduction and mutation, among others. The main objective is then to search in the population for the individuals with the best characteristics to combine them and form even better individuals until sufficient time has passed (a number G of generations) or a satisfactory solution is found [14]. For a more detailed discussion about GAs see [5, Section 2B].

The PSO algorithm is a stochastic optimization technique based on simulating animal social behavior. It works by having a population (the swarm) of individuals (particles) representing possible solutions to a problem. Each particle remembers their optimal position and velocity, defined by their fitnesses $f_{fit}(\cdot)$, as well as those of the swarm as they move in the search space [16]. Each generation combines the particle's information in order to adjust their velocities which are then used to compute their new positions as they change their state until they reach the optimal state or sufficient time has passed [16].

In this work, considering a GA population or PSO swarm of individuals and particles consisting in a network realization, the fitness function $f_{fit}(\cdot)$ is defined as the sum of each link SE. Therefore we maximize the overall bit rate, calculated as discussed in Subsection II-B per unit of bandwidth.

III. Results and Analysis

For the simulations, we considered a region R with area $0.49\,\mathrm{km}^2$ with $C = 10$ cells, where L was calculated from the link budget for the proposed scenario. We calculate for the strictest regime, i.e., $d_{k,m} \geq d_2$, the target signal noise ratio (SNR) of 0 dB at the cell edge, the average distance for each scenario, thus a parameterized distance for the proposed study. A total number of $K = 60$ UEs is distributed both inside and outside $N = 3$ hotspots following Algorithm 1 over the region R. Variable percentages p% of the BSs are considered to be IAB nodes with the remaining $(100 - p)\%$ of them becoming IAB donors. A shadowing standard deviation of σ_S = 8 dB is considered, while the noise power, IAB donor and IAB nodes transmit power were $-91\,\mathrm{dBm}$, $35\,\mathrm{dBm}$, $24\,\mathrm{dBm}$ respectively.

Each scenario was optimized for $S = 40$ snapshots independently, i.e. independent Monte Carlo realizations, and each realization was comprised of populations of $P = 100$ individuals evolving along $G = 100$ generations/iterations. The GA optimization parameters were, as in [5], single cutting point crossover, roulette wheel for the parent selection, and a 0.4% mutation rate. As for the PSO, the inertial weight, cognitive or persistence factor, and the social factor were 1, 1, and 2, respectively, as in [9]. The most important simulation parameters are presented in Table I.

In Fig. 2, the median SEs of all generations of GA and iterations of PSO is shown. Each graph shows the percentage p of IAB nodes for GA and PSO, where the solid curve represents the values reached at the 50° percentile for both algorithms, while the corresponding surrounding light regions refer to the standard deviations obtained in the simulations.

It is important to note that for all the percentages p simulated, both algorithms start approximately with the same average SE range. We can see that for the three simulated scenarios, GA and PSO perform quite similarly, with GA being a bit better except for the $p = 70\%$ scenario. This likely happened because for higher IAB node percentages the network becomes more susceptible to the propagation phenomena as modeled by (7), meaning IAB nodes need to be positioned more closely to their donors in order to avoid bad

TABLE I

SIMULATION ASSUMPTIONS.

Parameter	Symbol	Value
Grid		
Coverage area	R	$0.49\,\mathrm{km}^2$
Number of BSs	C	10
Percentage of IABs nodes	p	30%, 50%, 70%
Number of UEs	K	60
Number of hotspot UEs		20
Number of hotspots	N	3
Monte Carlo realizations	S	40
Link and propagation		
Path loss	$L_{k,m}(d_{k,m})$	Cf. (1)
Shadowing	σ_s	8 dB
Shadowing parameter	ϵ	0.5
Fast fading	$h_{i,j}$	Cf. (4)
IAB donor power	$10\log_{10}(p_{i,j})$	35 dBm
IAB node power	$10\log_{10}(p_{i,j})$	24 dBm
AWGN power	$10\log_{10}(\sigma_n^2)$	-91 dBm
genetic algorithm		
Number of individuals	P	100
Number of generations	G	100
Fitness	$f_{fit}(\cdot)$	Sum of SEs
Mutation rate	α_m	0.4% [14]
Crossover parent selection	—	Roulette wheel [5]
Reproduction rule	—	Single cutting point [5]
particle swarm optimization		
Number of particles	P	100
Number of iterations	G	100
Fitness	$f_{fit}(\cdot)$	Sum of SEs
Inertia weight	ω	1 [9]
Persistence	c_1	1 [9]
Social influence	c_2	2 [9]

backhaul links, while at the same time there are fewer IAB donors simplifying their positioning, which leads to an easier PSO process.

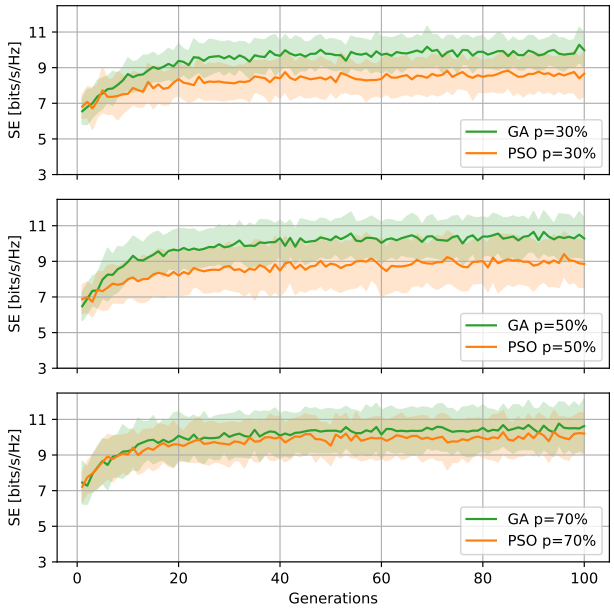

Fig. 2. Median SE over 40 Monte Carlo snapshots along of the generations/iterations of GA/PSO algorithms.

TABLE II

MEDIAN SES FOR EACH SCENARIO AT THE LAST GENERATION.

IAB nodes percentage	30%	50%	70%
GA [bits/s/Hz]	9.98	10.28	10.63
PSO [bits/s/Hz]	8.66	8.85	10.21

Quantitatively, for the GA optimization, the ideal median SEs per BS obtained was approximately $9.98\,\mathrm{bits/s/Hz}$, $10.28\,\mathrm{bits/s/Hz}$ and $10.63\,\mathrm{bits/s/Hz}$ for $p = 30\%$, $p = 50\%$ and $p = 70\%$, respectively, while for PSO they were $8.66\,\mathrm{bits/s/Hz}$, $8.85\,\mathrm{bits/s/Hz}$ and $10.21\,\mathrm{bits/s/Hz}$ in the same order, as shown in Table II. Based on these results, we can see that there is an initial percentage difference of 13% for the first two scenarios analyzed, while for the last one, there is a difference of around 3% between the SE obtained via GA and PSO.

In Fig. 3 the 50° percentile of SINRs obtained for GA and PSO, green and orange bars, per scenario are shown. We also include the median SINR of a random BS deployment, the blue bar, as a representation of an unplanned BS placement.

It is possible to note that the median SINR for the random deployment were approximately $1.29\,\mathrm{dB}$, $1.74\,\mathrm{dB}$ and $2.79\,\mathrm{dB}$ for $p = 30\%$, $p = 50\%$ and $p = 70\%$, respectively. Analogously, the PSO median SINR values were $26.07\,\mathrm{dB}$, $26.64\,\mathrm{dB}$ and $30.71\,\mathrm{dB}$ for $p = 30\%$, $p = 50\%$ and $p = 70\%$, while the GA algorithm obtained the highest median SINR values: $30.04\,\mathrm{dB}$, $30.95\,\mathrm{dB}$ and $31.99\,\mathrm{dB}$ in the same order.

We can see that both algorithms perform a lot better than the unplanned case, as expected, increasing the median SINR by at least $24.77\,\mathrm{dB}$, a huge improvement. The difference in performance between GA and PSO was not as significant, being $3.97\,\mathrm{dB}$, $4.31\,\mathrm{dB}$ and $1.27\,\mathrm{dB}$ for $p = 30\%$, $p = 50\%$ and $p = 70\%$, respectively, showing once again that the PSO algorithm performance improved for the $p = 70\%$ scenario.

Therefore, as shown in Fig. 3, Fig. 2 and Table II, both PSO and GA proved to be quite effective planning tools, shown to provide large gains compared to an unplanned deployment.

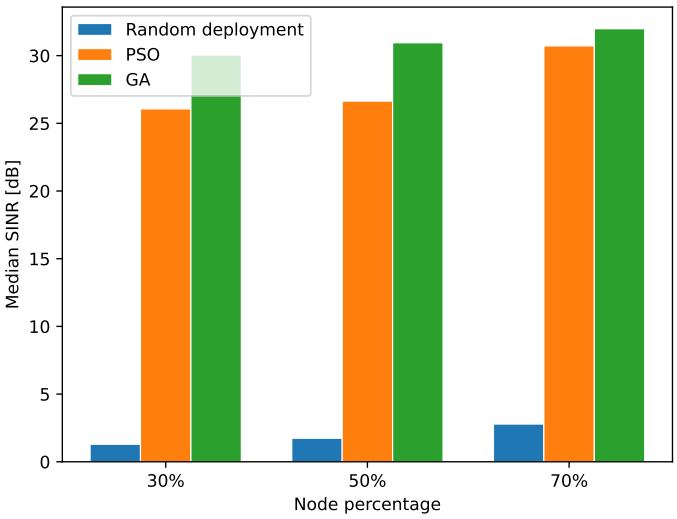

Fig. 3. Median SINRs obtained for GA/PSO and random deployment per scenario.

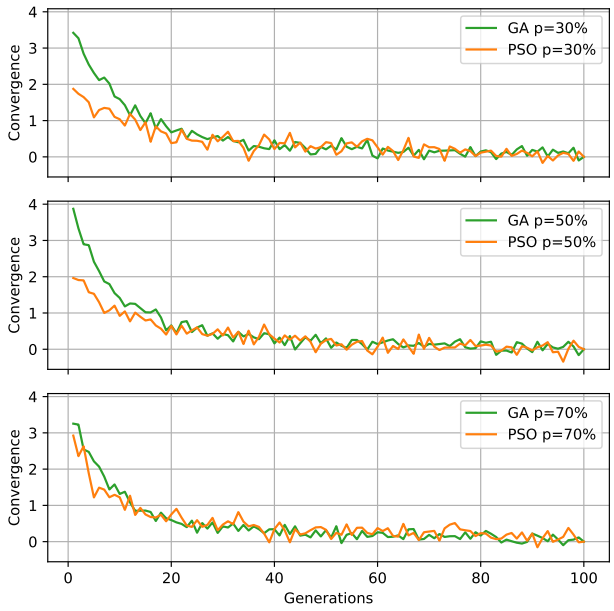

Fig. 4. Convergence obtained for the median GA/PSO algorithms generations/iterations in each scenario.

In Fig. 4 the convergences of the median iterations of the GA and PSO algorithms, green and orange curves, respectively, are shown for each scenario $p = 30\%$, $p = 50\%$ and $p = 70\%$. The convergence metric is taken as the difference between the generation maximum SE and the final result of the optimization process. In all scenarios, we can notice that the PSO algorithm converges faster than the GA, but, as we increase the percentage p of IAB nodes, their behaviour becomes more similar, as we have also observed in Fig. 2 and Fig. 3.

So, despite achieving lower results overall, specially for lower percentages of IAB nodes, PSO is still a viable option, since it was found to be more efficient in that it tends to have better convergence as shown in Fig. 4, and also in a plethora of different problems [17].

Interestingly, in Fig. 2 we can see that as the percentage p of IAB nodes increases the same happens with the SEs, which likely occurs due to the lower interference caused by the lower power of IAB nodes which was also observed in [5]. This evidences once more the suitability of IAB networks as a way of providing more flexibility and cost-effectiveness when deployed with careful planning.

IV. Conclusions

In this work, the performance of two EA, GA and PSO, for SOOP were compared, considering BSD of an IAB network as the optimization problem and the median SE per BS and SINR as the quality metrics. It was possible to conclude that, despite the higher SE generated by GA, the PSO algorithm proved to be also a good option due of its efficiency. There is no single optimal heuristic algorithm for the BSD problem addressed in this work, each one having its own trade-offs, given the complexity of the problem in question and the efficiency of the algorithms for different optimization scenarios.

It was also discussed that as the number of lower power IAB nodes increased, network performance improved likely due to the lower interference, which prompts us to consider, as a future perspective, the analysis not only of the BSD but also the energy efficiency of IAB networks, in the optimization process. Furthemore in this work only a random strategy was used for BSD, leaving other more realistic approaches to be used in future works.

Another future perspective is to analyze the robustness of the techniques used here in scenarios with more realistic and channel state information (CSI) to investigate more closely the suitability of the usage of heuristics as real network planning tools.

Acknowledgements

The authors would like to thanks the Wireless Telecommunications Research Group (GTEL) for sharing their computational resources for the development of this work.

References

[1] F. Jejdling, “Ericsson mobility report,” Ericsson, TR, 2023.
[2] V. F. Monteiro, F. R. M. Lima, D. C. Moreira, D. A. Sousa, T. F. Maciel, B. Makki, and H. Hannu, “Paving the way towards mobile iab: Problems, solutions and challenges,” arXiv:2206.14946, 2022.
[3] 3GPP, “Evolved universal terrestrial radio access (e-utra); relay architectures for e-utra (lte-advanced),” std3GPP, techreport 36.806, Apr. 2010.
[4] M. Polese, M. Giordani, T. Zugno, A. Roy, S. Goyal, D. Castor, and M. Zorzi, “Integrated access and backhaul in 5G mmWave networks: Potential and challenges,” vol. 58, no. 3, p. 62–68, Mar. 2020.
[5] F. I. G. Carvalho, T. F. Maciel, R. V. O. de Paiva, and I. B. Palhano, “Genetic algorithm for base station placement in integrated access and backhaul networks,” in *Workshop on Communication Networks and Power Systems (WCNPS)*, 2023, p. 1–7.
[6] C. Madapatha, B. Makki, A. Muhammad, E. Dahlman, M.-S. Alouini, and T. Svensson, “On topology optimization and routing in integrated access and backhaul networks: A genetic algorithm-based approach,” *IEEE Open Journal of the Communications Society*, vol. 2, p. 2273–2291, 2021.
[7] O. P. Adare, H. Babbili, C. Madapatha, B. Makki, and T. Svensson, “Uplink power control in integrated access and backhaul networks,” in *2021 IEEE International Symposium on Dynamic Spectrum Access Networks (DySPAN)*, 2021, p. 163–168.
[8] M. B. Pereira, F. R. P. Cavalcanti, and T. F. Maciel, “Particle swarm optimization for base station placement,” in *2014 International Telecommunications Symposium (ITS)*, 2014, p. 1–5.
[9] M. B. Pereira, “Particle swarm optimization and differential evolution for base station placement with multi-objective requirements,” thesis, Federal University of Ceará, 2015.
[10] F. Aurenhammer, “Voronoi diagrams—a survey of a fundamental geometric data structure,” *ACM Comput. Surv.*, vol. 23, no. 3, p. 345–405, sep 1991.
[11] I. M. Braga, R. P. Antonioli, G. Fodor, Y. C. B. Silva, and W. C. Freitas, “Decentralized joint pilot and data power control based on deep reinforcement learning for the uplink of cell-free systems,” *IEEE Transactions on Vehicular Technology*, vol. 72, no. 1, 2023.
[12] Özlem Tugfe Demir, E. Björnson, and L. Sanguinetti, *Foundations of User-Centric Cell-free Massive MIMO*, 2021.
[13] T. M. Cover and J. A. Thomas, *Elements of Information Theory (Wiley Series in Telecommunications and Signal Processing)*. USA: Wiley-Interscience, 2006.
[14] R. Linden, *Algoritmos Geneticos*. CIENCIA MODERNA, 2012.
[15] J. Kennedy and R. Eberhart, “Particle swarm optimization,” in *Proceedings of ICNN’95 - International Conference on Neural Networks*, vol. 4, 1995, p. 1942–1948 vol.4.
[16] D. Wang, D. Tan, and L. Liu, “Particle swarm optimization algorithm: an overview,” *Soft Computing*, vol. 22, no. 2, p. 387–408, Jan. 2017. [Online]. Available: http://dx.doi.org/10.1007/s00500-016-2474-6
[17] R. Hassan, B. Cohanim, O. De Weck, and G. Venter, “A comparison of particle swarm optimization and the genetic algorithm,” in *46th AIAA/ASME/ASCE/AHS/ASC structures, structural dynamics and materials conference*, 2005, p. 1897.